Optimization of congo red removal by adsorption onto $NiFe_2O_4$/GO nanocomposite

Van Thuan Tran[1], Van Thinh Pham[2,3], Thi Phuong Quynh Bui[4], Duy Trinh Nguyen[1], Long Giang Bach[1*]

[1]*Nguyen Tat Thanh University, Ho Chi Minh city, Vietnam*
[2]*Dong Nai Technology University, Dong Nai province, Vietnam*
[3]*Graduate University of Science and Technology, Vietnam Academy of Science and Technology*
[4]*Ho Chi Minh city University of Food Industry, Vietnam*

Received 14 June 2017; accepted 11 September 2017

Abstract:

The present study focused on the use of the magnetic nanocomposite $NiFe_2O_4$/GO (GO - Graphene oxide) as an efficient adsorbent for the removal of congo red (CR). The $NiFe_2O_4$/GO was synthesized from $NiFe_2O_4$ and GO via a facile route, and the structure of this nanocomposite was analyzed by X-ray powder diffraction (XRD), scanning electron microscope (SEM), and Vibrating sample magnetometer (VSM). By applying the response surface methodology, the profound relationship was found between variables (initial concentration, adsorbent dosage, and pH) and CR removal efficiency. Moreover, the model was optimized to give a favourable condition for the adsorption. Up to 94.7% of CR removal was obtained via a confirmation test, and this result indicated that the magnetic $NiFe_2O_4$/GO was a promising material in terms of treatment for CR-contaminated wastewater.

Keywords: *congo red, $NiFe_2O_4$/GO, optimization, response surface methodology.*

Classification number: *2.2*

Introduction

Nowadays, environmental pollution has increasingly become a universal issue as a consequence of the discharge of many hazardous chemicals [1]. Among the pollutants, organic dyes contribute to a large proportion because their contamination in wastewater often originates from fundamental and widespread industries such as textile [2]. Such compounds at high concentrations are considered as toxic sources due to toxicological and aesthetical reasons, and thus they are able to cause carcinogenic effects [3]. Meanwhile, these organic pollutants can accumulate a great amount in the environment over a period of time and result in persistent pollutions because of their low biodegradability [4]. CR is a crucial representative of secondary diazo anionic dyes, which leads to an allergic reaction and will be metabolized to benzidine, a human carcinogen [5]. Therefore, it is strongly expected to develop an eco-friendly method for treatment of CR-bearing wastewater.

Over the past years, some feasible approaches for the removal of dyes have been reported such as various physical, chemical, and biological methods, including adsorption, biosorption coagulation/flocculation, catalytic reduction, electrolytic reduction membrane filtration, and liquid-liquid extraction [6]. Although the aforementioned methods generally remain their own limitations towards either cost-effectiveness or performance, adsorption is a highly effective separation technique because its advantage is superior to that of other methods in terms of initial cost, simplicity, good operation, and cyclability [7]. There are various kinds of common adsorbents which can be highly compatible with adsorption systems. However, adsorbents need to be reusable towards "green chemistry" trend and can be easily separated from the aqueous solution, so we have developed a class of nickel-based spinel ferrite magnetic material $NiFe_2O_4$ [8]. To enhance the surface properties by means of adding various functional groups, graphene oxide can be loaded to modify a rigid structure of $NiFe_2O_4$ and form a nanocomposite $NiFe_2O_4$/GO [9]. These types of materials can, therefore, be easy to perform magnetic separation and recycling as they hold unique properties of facile synthesis, magnetic recoverability and stability.

The present work aims to show the influential factors including initial CR concentration, the dosage of $NiFe_2O_4$/GO, and pH of the solution on the removal of CR by adsorption onto $NiFe_2O_4$/GO using the response surface methodology (RSM). The second-order RSM-based polynomial regression model was used

*Corresponding author: Email: blgiang@ntt.edu.vn

to evaluate the mathematical relationship of factors and find the optimum region for removal of dye ions.

Materials and methods

Chemicals and instruments

All chemicals for this study were commercially purchased from Merck. The XRD was implemented on D8 Advance Bruker powder diffractometer with a Cu-Kα excitation source. The SEM was recorded with the Japanese instrument S4800 and used an accelerating voltage source of 10 kV with a magnification of 7000. The magnetic properties were determined by VSM.

Production of $NiFe_2O_4$/GO

$NiFe_2O_4$ and GO were performed by a two-step procedure as early reported [8, 10]. In the typical experiment, a beaker containing 1.0 g of $NiFe_2O_4$ 50 ml in 50 ml ethanol and another beaker containing 5 ml of GO colloidal suspension in 45 ml of water were put in an ultrasonic bath for one hour. After heating to 60°C, the mixtures were transferred into a 500 ml beaker and then stirred to vaporize. The solid was dried at 90°C and used for the present study.

Adsorption batch

The $NiFe_2O_4$/GO (0.16-1.84 g/l) was poured into an Erlenmeyer flask containing 50 ml of CR solution (66.4-133.6 mg/l). After the absorption equilibrium in three hours, the solid was removed from the mixture. The residual concentrations were confirmed by AAS. Twenty experiments were performed by using central composite design (CCD) (Table 1) at five levels including the low (encoded -1), high (encoded +1), and rotatable (encoded ± 1.68).

Table 1. Independent variables matrix and their encoded levels.

No	Independent factors	Code	Levels				
			-1.68	*-1*	*0*	*+1*	*+1.68*
1	CR concentration (mg/l)	x_1	66.4	80	100	120	133.6
2	$NiFe_2O_4$/GO dosage (g/l)	x_2	0.16	0.5	1.0	1.5	1.84
3	pH (-)	x_3	3.6	5	7	9	10.4

Results and discussions

Textural characterization of $NiFe_2O_4$/GO

It can be seen from Fig. 1A that the typical peak of GO at a low angle of $2\theta = 10.8^0$ was absent from the given diagram [11]. This phenomenon can be explained as follows: the graphene oxide was remarkably reduced through the oxidative reaction, where new bonds between graphene oxide and active open-metal sites of the $NiFe_2O_4$ were formed [8-11]. Moreover, other shape diffraction peaks at 26.4°, 30.4°, 35.8°, 43.4°, 63.0° revealed the crystalline nature which fitted well with spinel structure of ferrites reported by a previous study [9].

Figure 1B showed that the saturation magnetization value was 2.38 emu/g, which was considered to be significantly lower than that of the previous report [8]. Magnetization decrease could be attributable to the presence of non-magnetic graphene loaded on the surface of ferrite $NiFe_2O_4$ in the preparation of $NiFe_2O_4$/GO [1]. The SEM image at various scales of 500 nm in Fig. 1C revealed the morphological property from $NiFe_2O_4$/GO. Obviously, the $NiFe_2O_4$/GO possesses a type of porous and defective surface. The average diameter of nanoparticles was calculated to be from 40 to 50 nm.

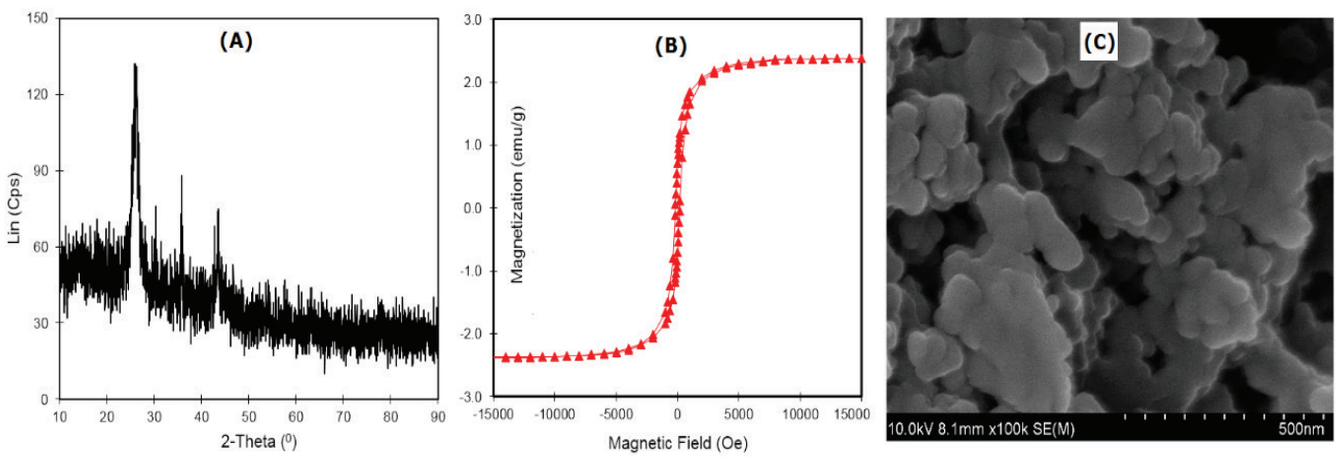

Fig. 1. XRD spectra (A), VSM (B), and SEM image (C) of the $NiFe_2O_4$/GO.

Table 2. The matrix of observed and predicted values.

No	Variables			Response	
	x_1 (C_i, ppm)	x_2 (dosage, g/l)	x_3 (pH)	Actual (%)	Predicted (%)
1	80	0.5	5	43.9	45.6
2	120	0.5	5	30.3	29.0
3	80	1.5	5	91.9	93.8
4	120	1.5	5	80.8	84.0
5	80	0.5	9	56.8	56.0
6	120	0.5	9	42.4	42.9
7	80	1.5	9	60.4	70.1
8	120	1.5	9	62.9	63.7
9	66.4	1	7	80.2	77.5
10	133.6	1	7	59.0	58.2
11	100	0.16	7	18.5	19.5
12	100	1.84	7	90.8	77.5
13	100	1	3.6	74.0	71.9
14	100	1	10.4	70.0	63.6
15	100	1	7	71.0	73.8
16	100	1	7	75.8	73.8
17	100	1	7	73.7	73.8
18	100	1	7	76.6	73.8
19	100	1	7	73.1	73.8
20	100	1	7	72.1	73.8

Table 3. ANOVA for response surface quadratic model.

Source	Sum of squares	Degree of freedom	Mean square	F-value	Prob. > F	Comment
Model	6393.26	9	710.36	77.88	< 0.0001[s]	SD = 3.02
x_1	44840	1	448.40	49.16	< 0.0001[s]	Mean = 64.82
x_2	4057.32	1	4057.32	444.81	< 0.0001[s]	CV(%) = 4.66
x_3	82.35	1	82.35	9.03	0.0132[s]	Press = 563
$x_1 x_2$	22.44	1	22.44	2.46	0.1478[n]	R^2 = 0.9859
$x_1 x_3$	5.78	1	5.78	0.63	0.4445[n]	$R^2_{(adj.)}$ = 0.9733
$x_2 x_3$	584.82	1	584.82	64.11	< 0.0001[s]	AP = 34.767
x_1^2	63.48	1	63.48	6.96	0.0248[s]	
x_2^2	1151.82	1	1151.82	126.27	< 0.0001[s]	
x_3^2	65.64	1	65.64	7.20	0.0230[s]	
Residuals	91.22	10	9.12			
Lack of Fit	68.19	5	13.64	2.96	0.1293[n]	
Pure Error	23.03	5	4.61			

[s]significant at $p < 0.05$; [n]not significant at $p > 0.05$.
ANOVA: Anlysis of variance.

Assessment of experimental results with DX10

To investigate a wide range of parameters (Table 2), the table for response and predicted values was applied by the Design-Expert 10 (DX10). This table gives information about actual experiments obtained by independent runs and the predicted values (via DX10) built from these true runs. In this study, there were 20 actual runs including 14 fluctuation experiments of three variables and six replications at the central point. A proposed model was considered to be highly fitted with actual data if its parameters from ANOVA table satisfied a series of mentioned conditions: (1) Correlation coefficient (R^2) approaches 1.0; (2) Values of P or P-values are lower than 0.05 at 95% confidence level; (3) Adequate precision (AP) ratio is greater than 4.0; (4) Lack-of-fit value is higher than 0.05. It is inevitable that all the above standards met these requirements (Table 3). Moreover, Fig. 2A and Fig. 2B showed that the predicted values versus actual values distributed on the straight line and the residuals versus runs plot demonstrated that the obtained results of total 20 runs were experimentally random. Therefore, the proposed model was statistically significant.

Effect of independent variables on the removal of CR

Figure 2C shows "desirability" of the model, in which the experiments could be possible to obtain the highest results (probability = 100%) if they were conducted by the optimization condition. The region of maximum "desirability" was obviously spreading, thus it allowed obtaining good CR removal efficiencies. To describe the optimal regions that were plotted by altering two variables and holding another at zero level, the response surfaces were drawn and shown in Fig. 3.

To begin with, three-dimensional response surfaces were firstly plotted in Fig. 3A. The CR removal efficiency would rise by increasing the amount of $NiFe_2O_4$/GO. The main cause for this phenomenon was that when adding the $NiFe_2O_4$/GO into the solution, the number of active adsorption sites rose to create more functional groups. Consequently, an optimum zone was positioned at the higher side of dosage. Meanwhile, the initial concentration of CR anions had a negligible impact on the CR removal efficiency.

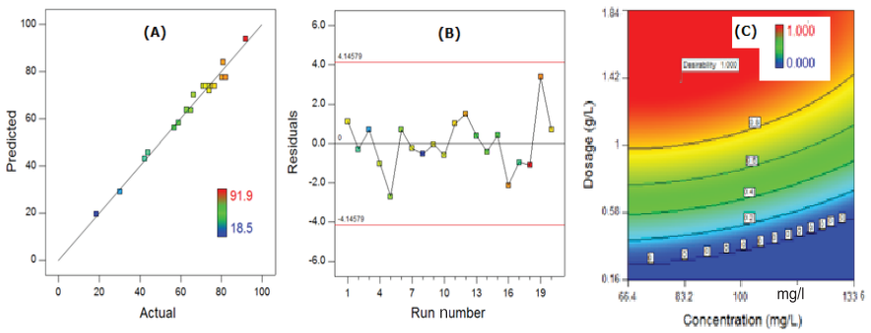

Fig. 2. Actual plot versus predicted plot (A), residuals versus runs (B), and "desirability" (C).

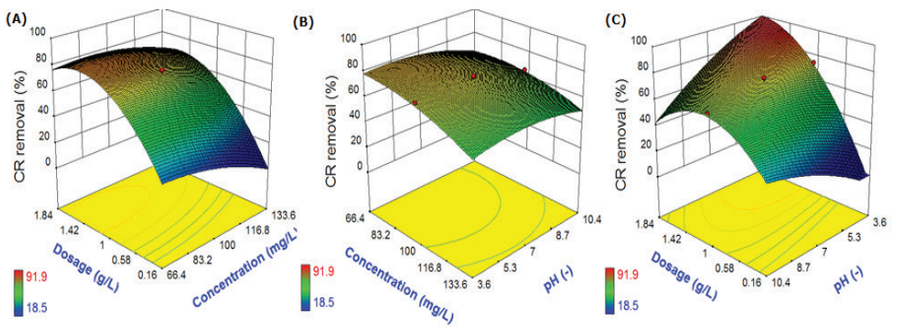

Fig. 3. Surface response plot (A-C) for the removal of CR by $NiFe_2O_4$/GO.

Table 4. Model confirmation.

C_i (mg/l)	Dosage (g/l)	pH (-)	Desirability	Ni^{2+} removal (%)	
				Predict	*Test*
82.2	1.4	4.0	1.00	94.3	94.7

Figure 3B indicated a significant effect of initial concentration and pH on CR removal efficiency. In contrast, there was a strong interaction between dosage and pH against the percentage of CR removal. The CR was markedly removed from the aqueous solution at a high level of dosage and low level of pH (Fig. 3C). When pH in solution decreased, the material surface would be charged positively. Thus, new bonds between positive-charged material and CR anions were favourably formed to enhance the adsorption.

The predicted optimal-condition-based model experiment was further conducted to verify the suitability of the proposed model: C_i = 82.2 mg/l, dosage = 1.4, and pH = 4.0 with the highest desirability of 1.0 (Table 4). Thereby, the test for the percentage of CR removal was obtained at 94.3%, which was nearly closed to the predicted value of 94.7 %. This result demonstrated the high compatibility of the proposed models with the experimental data.

Conclusions

The porous magnetic nanocomposite $NiFe_2O_4$/GO was successfully synthesized and characterized by several techniques. The results indicated that the $NiFe_2O_4$/GO had a highly crystalline nature with defective structure. By evaluating parameters from ANOVA, the proposed model was proved to be statistically significant. Moreover, the DX10 obtained the optimal condition for the removal of CR from solution at Ci = 82.2 mg/l, dosage = 1.4, and pH = 4.0. With a high result of removal efficiency (94.7%), the $NiFe_2O_4$/GO was an efficient adsorbent to remove the CR from contaminated groundwater.

REFERENCES

[1] W. Yin, H. Cao (2017), "Solvothermal synthesis of magnetic $CoFe_2O_4$/rGO nanocomposites for highly efficient dye removal in wastewater", *RSC Adv.*, **7**, pp.4062-4069.

[2] S. Han, K. Liu, Y. Zhu (2017), "Superior Adsorption and Regenerable Dye Adsorbent Based on Flower-Like Molybdenum Disulfide Nanostructure", *Sci. Rep.*, **7,** pp.43-59.

[3] Ghanizadeh (2011), "Adsorption kinetics and isotherm of methylene blue and its removal from aqueous solution using bone charcoal", *React. Kinet. Mech. Catal.*, **102(1),** pp.127-142.

[4] L. Ai, Z. Chen (2011), "Removal of methylene blue from aqueous solution by a solvothermal-synthesized graphene/magnetite composite", *J. Hazard. Mater.*, **192(3)**, pp.1515-1524.

[5] V.K. Gupta, S. Suhas (2009), "Application of low-cost adsorbents for dye removal - A review", *J. Environ. Manage.*, **90(8)**, pp.2313-2342.

[6] Q. Zhao, H. Zhao, T. Jiang (2017), "Efficient Removal of Pb(II) from Aqueous Solution by $CoFe_2O_4$/Graphene Oxide Nanocomposite: Kinetic, Isotherm and Thermodynamic", *J. Nanosci. Nanotechnol.*, **17(6)**, pp.28-31.

[7] A.A. Inyinbor, G.A. Olatunji (2016), "Kinetics, Isotherms and thermodynamic modeling of liquid phase adsorption of Rhodamine B dye onto Raphia hookerie fruit epicarp", *Water Resour. Ind.*, **15**, pp.14-27.

[8] S. Yáñez Vilar, M. Sánchez-Andújar, C. Gómez-Aguirre, J. Mira, M.A. Señarís Rodrígueza, S. Castro García (2009), "A simple solvothermal synthesis of MFe_2O_4 (M = Mn, Co and Ni) nanoparticles", *J. Solid State Chem.*, **182(10)**, pp.2685-2690.

[9] K. Hareesh, S.D. Dhole (2016), "PSS wrapped $NiFe_2O_4$/rGO tertiary nanocomposite for the super-capacitor applications", *Electrochim. Acta.*, **201**, pp.106-116.

[10] C. Tan, X. Huang, H. Zhang (2013), "Synthesis and applications of graphene-based noble metal nanostructures", *Materialstoday.*, **16(1-2)**, pp.29-36.

[11] F. Hongbin, L. Yueming, L. Jinghong (2012), "Strong reduced graphene oxide-polymer composites: hydrogels and wires", *RSC Adv.*, **2**, pp.6988-6993.